Bulk and Surface Properties of Maleimide Copolymers: Effect of Fluorinated Side Chains

Dietmar Appelhans,* Zhong-Gang Wang, Stefan Zschoche, Rong-Chuan Zhuang, Liane Häussler, Peter Friedel, Frank Simon, Dieter Jehnichen, Karina Grundke, Klaus-Jochen Eichhorn, Hartmut Komber, and Brigitte Voit

Leibniz Institute of Polymer Research Dresden, Hohe Strasse 6, D-01069 Dresden, Germany

Received July 5, 2004; Revised Manuscript Received November 16, 2004

ABSTRACT: We studied the bulk and surface properties of maleimide (MI) copolymers based on three different main chains, poly(ethene-*alt*-maleimide), poly(styrene-*alt*-maleimide), and poly(octadecene-*alt*-maleimide), with two different types of side chains (4-(*N*-perfluoroheptylcarbonyl)aminobutyl and *n*-dodecyl). By the given alternating substitution pattern of the side chains in MI copolymers, different side chain organizations caused different surface energetics. On the basis of determined advancing contact angles of water on spin-coated MI copolymer films, solid surface tensions γ_{sv} were calculated in the range of 19−23 mJ/m^2 for alkyl side chains and of 11−18 mJ/m^2 for fluorinated side chains. In both cases, within the aliphatic and fluorinated series, the main chain poly(styrene-*alt*-maleimide) suppressed a better alignment of side chains resulting in nondensely packed CH_3 and CF_3 surface groups, respectively, and higher solid surface tensions. For this study small- and wide-angle X-ray diffraction, differential scanning calorimetry, attenuated total reflection infrared spectroscopy, ellipsometry, atomic force microscopy, contact angle measurements, angle-resolved X-ray photoelectron spectroscopy, and molecular modeling calculation were used to investigate the bulk and surface properties.

Introduction

The great challenge of the design of various bulk or surface properties is connected with the use of a nonchanging polymeric backbone. This can be realized by the exchange of attached side chains to receive the desired characteristic features of such polymeric materials. For this purpose the polymer analogous modified alternating maleic anhydride copolymer fulfills all the desired characteristic structure abilities to realize copolymer series possessing one or various side chains. Thus, a great variety of alternating maleimide (MI) copolymers was achieved to result in different material, bulk, and surface properties starting from helical-organized polymeric backbones[1] over nonlinear optical properties,[2] image recording materials,[3] hydrophilic[4] and hydrophobic[5] surfaces, supramolecular polymer interactions,[6] biocompatible surfaces,[7] liquid crystallization,[8] and extraction properties[9] to (multi)layer formation by the Langmuir−Blodgett technique[10] and many more.

The background of the simple modification of alternating maleic anhydride copolymers into the corresponding MI copolymers inspired us to investigate structure−property relationships of MI copolymers with aliphatic and fluorinated side chains for surface engineering to design different states of hydrophobic surfaces. Especially, we are interested in the formation of exposed CF_3 and CH_3 groups on the top of copolymer surfaces and its resulting wettability behavior and surface tension after thermal treatment as an additional modification step to achieve higher states of hydrophobicity. MI copolymers with six different chemical structures were synthesized by polymer analogous reactions of maleic anhydride copolymers with amino-functionalized compounds, shown in Scheme 1, for this purpose.

Scheme 1

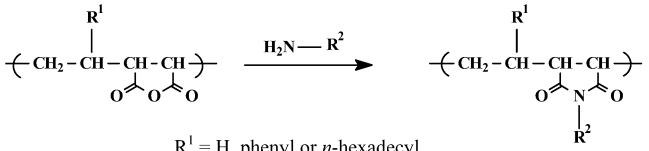

R^1 = H, phenyl or *n*-hexadecyl
R^2 = R_f (-$(CH_2)_4$-NH-CO-C_7F_{15}) or
R_h (-$(CH_2)_{11}CH_3$)

ETMF: R^1 = H and R^2 = R_f ETMH: R^1 = H and R^2 = R_h
STMF: R^1 = phenyl and R^2 = R_f STMH: R^1 = phenyl and R^2 = R_h
ODMF: R^1 = *n*-hexadecyl R^2 = R_f ODMH: R^1 = *n*-hexadecyl and R^2 = R_h

Poly(ethene-*alt*-*N*-(*n*-dodecyl)maleimide) (ETMH), poly(styrene-*alt*-*N*-(*n*-dodecyl)maleimide) (STMH), and poly(octadecene-*alt*-*N*-(*n*-dodecyl)maleimide) (ODMH) with aliphatic side chains were synthesized. The fluorinated copolymers possess a defined perfluoroalkyl (R_f) side chain (4-(*N*-perfluoroheptylcarbonyl)aminobutyl) whereby three different backbones, poly(ethene-*alt*- maleimide) in ETMF, poly(styrene-*alt*-maleimide) in STMF, and poly(octadecene-*alt*-maleimide) in ODMF, were used. STMF and STMH have an additional phenyl substituent, and ODMF and ODMH have a hexadecyl substituent. The hexadecyl substituent can be regarded as a second side chain in ODMF and ODMH. Thus, it was possible to study the structure−property relationships of alternating MI copolymers in the bulk and on the surface in detail: a focus related to the influence of the main chain and the influence of the side chain on the bulk and surface properties.

Different results of surface properties from the literature are known. Del Rio et al.,[5a] Grundke et al.,[5b] and Kwok et al.[11] have done first investigations of the influence of aliphatic side chains in alternating MI coplymers on the wettability of these surfaces. Especially, Grundke et al. focused on the exchange of two main chain derivatives. Thus, it could be shown that after the incorporation of longer aliphatic side

* To whom correspondence should be addressed: Tel ++49 351 4658 353; Fax ++49 351 4658 565; e-mail applhans@ipfdd.de.

10.1021/ma0486492 CCC: $30.25
Published on Web 02/03/2005

chains (C_8 and C_{12} alkyl chain) in poly(propene-*alt*-*N*-alkylmaleimide)s or poly(styrene-*alt*-*N*-alkylmaleimide)s the surface tension is essentially equal caused by shielding of the polar backbone chain. Therefore, similar results for MI copolymers with longer aliphatic side chains were received. From the low surface tension values of about 23 mJ/m^2, a nearly perfectly organized exposition of CH_3 groups on the top of polymer layers is assumed.[5b]

Another important result of the MI homo- and copolymers is the realization of defined layer distances in the bulk phase.[1,5b,12,13] The layer distances can be explained by the presence of helical main chain conformation and possible side chain interdigitation. For the helical main chain conformation in alternating MI copolymers *trans*-configurated succinimide rings in the main chain are required after successful conversion of predominately *trans*-configurated maleic anhydride rings[14−16] with amino-functionalized compounds.

Only alternating MI copolymers were used to realize preferentially exposed CH_3 or CF_3 groups on the top of the surface. The resulting MI copolymers offer the unique chance to compare, especially, the influence of changing backbones with two different attached side chains on the surface properties. The use of polymer analogous reaction allows us to obtain MI copolymers with the same main chain and the same degree of polymerization, but different functionalities due to attached side chains via the N atom of the maleimide ring. For these comparisons small-angle X-ray diffraction (SAXS), wide-angle X-ray diffraction (WAXS), differential scanning calorimetry (DSC), and attenuated total reflection infrared spectroscopy (ATR-IR) were used to investigate the bulk properties. Ellipsometry, atomic force microscopy (AFM), contact angle measurements, and angle-resolved X-ray photoelectron spectroscopy (AR-XPS) were selected to investigate the surface properties. Molecular modeling was done to support the interpretation of the results for the bulk and surface properties. Especially, the wettability of copolymer films toward water was determined by contact angle measurements using the axisymmetric drop shape analysis profile (ADSA-P). Low-rate dynamic measurements from ADSA-P allow one to differentiate between thermodynamically relevant contact angles, i.e., contact angles which can be used in the Young equation, from very complex contact angle responses for some solid−liquid systems.[18] Constant advancing contact angles of water were used to calculate the solid surface tension by the equation-of-state approach for solid−liquid interfacial tensions.[17,18]

Experimental Section

Chemicals. Methyl perfluorooctanoate and hexafluoro-2-propanol were purchased by ABCR and used as received. Tetrahydrofuran (THF) and *n*-dodecylamine were purchased by ACROS and used as received. 1,4-Diaminobutane was purchased by Aldrich and used as received. The alternating maleic anhydride copolymers poly(ethene-*alt*-maleic anhydride) (MW 125 000 g/mol), poly(styrene-*alt*-maleic anhydride) (MW 20 000 g/mol), and poly(octadecene-*alt*-maleic anhydride) (MW 30 000−50 000 g/mol) were purchased by Aldrich (Munich), Leuna Werke AG (Germany), and Polyscience Inc. (Warrington, PA), respectively.

N-(4-Aminobutyl)perfluorooctaneamide Hydrochloride. 1,4-Diaminobutane (4.24 g, 48.13 mmol) was dissolved in 50 mL of dichloromethane under a nitrogen atmosphere. Methyl perfluorooctanoate (10.3 g, 24.1 mmol) was slowly added to the ice bath cooled reaction solution. After the addition of the ester the solution was kept at 0 °C for 1 h and then stirred at room temperature for 2 days. After that, the solvent was distilled off under vacuum, and the residual was suspended in diethyl ether and acidified with very diluted aqueous hydrogen chloride solution. The obtained solid was washed with diethyl ether and water sequentially and then dried in a vacuum oven at 40 °C for 2 days to yield 10.29 g (82.1%) of *N*-(4-aminobutyl)perfluorooctaneamide hydrochloride as white solid; mp 197.8−199.0 °C. ^{1}H NMR: δ = 1.53 (m, 4H, CH_2CH_2); 2.78 (t, 2H, CH_2NH_2*HCl); 3.22 (q, 2H, $R_fCONHCH_2$); 7.98 (s, 3H, CH_2NH_2*HCl); 9.59 ppm (t, 1H, R_fCONH). ^{13}C NMR: δ = 24.25 ($CH_2CH_2NH_2$*HCl); 25.36 (CO−$NHCH_2CH_2$); 38.30 (CH_2NH_2*HCl); 38.92 ($R_fCONHCH_2$); 105.0−120.0 (CF_2); 137.6 (CF_3); 156.63 ppm (R_fCONH). ^{19}F NMR: δ = −80.58 (CF_3), −118.78 (CF_2−CO), −121.77, −122.15, −122.57, −122.82, and −126.19 ppm (CF_2).

Aliphatic MI Copolymers ETMH, STMH, and ODMH. 1 mol of poly(ethene-*alt*-maleic anhydride), poly(styrene-*alt*-maleic anhydride), or poly(octadecene-*alt*-maleic anhydride) and 1.05 mol of *n*-dodecylamine were dissolved in THF and stirred at 120 °C for 24 h in an autoclave. The cooled reaction solution was poured into acidic water solution. The resulting MI copolymers ETMH, STMH, and ODMH were washed intensively with water and then dried in a vacuum oven at 40 °C. The copolymers were characterized by IR spectroscopy, proving complete conversion of the maleic anhydride ring into the maleimide ring. NMR investigation of the aliphatic MI did not reveal acid groups, too. Therefore, a nearly complete conversion of the maleic anhydride groups took place, and the degrees of attached side chains of converted maleic anhydride groups are shown in Table 1. The used reaction procedure is similar to previously described attempts.[5b]

Fluorinated MI Copolymers ETMF, STMF, and ODMF. 1 mol of poly(ethene-*alt*-maleic anhydride), poly(styrene-*alt*-maleic anhydride), or poly(octadecene-*alt*-maleic anhydride), 1.0 mol of *N*-(4-aminobut-1-yl)fluorooctaneamide hydrochloride, and 1.0 mol of triethylamine were dissolved in THF and stirred at 160 °C for 24 h in an autoclave. The cooled reaction solution was poured into acidic water solution. The resulting MI copolymers ETMF, STMF, and ODMF were washed intensively with water and then dried in a vacuum oven at 40 °C. The copolymers were characterized by IR spectroscopy, proving the conversion of the maleic anhydride ring into the maleimide ring. Also, fluorine analyses were done to calculate the degree of attached R_f side chains in MI copolymers. Table 1 shows the molecular weights of purchasable used poly(alkene-*alt*-maleic anhydride)s, degree of polymerized repeating units of alkene−maleic anhydride in used poly(alkene-*alt*-maleic anhydride)s, the found/theoretical data for F, and the degree of attached (R_f) side chains in MI. The chemical composition of MI copolymers will be shortly discussed in the XPS section and compared with fluorine analyses.

The NMR measurements were performed in 5 mm o.d. sample tubes with a Bruker DRX 500 NMR spectrometer operating at 500.13 MHz for ^{1}H, at 470.59 MHz for ^{19}F, and at 125.75 MHz for ^{13}C. DMSO-d_6 was used as solvent for all NMR experiments.

Table 1. Molecular Weight (M_w) of Converted Poly(alkene-*alt*-maleic anhydride)s (PAMA), Degree of Polymerization (P_n) for Repeating Unit Alkene−Maleic Anhydride in Used Poly(alkene-*alt*-maleic anhydride)s, the Theoretical/Found Data for F, and Calculated Degree of Attached Side Chains in MI

MI	M_w of PAMA × 10^3 g/mol	P_n	F[a] (wt %)	F[b] (wt %)	degree of side chains
ETMF	125	∼990	48.11	44.01	0.91[c]
ETMH	125	∼990			0.95−1[d]
STMF	20	∼100	42.64	40.50	0.95[c]
STMH	20	∼100			0.95−1[d]
ODMF	40	∼120	34.89	33.37	0.96[c]
ODMH	40	∼120			0.95−1[d]

[a] Theoretical data. [b] Obtained from fluorine analysis. [c] Based on found F content. [d] Based on ATR-IR results.

Fluorine elemental analyses were carried out by the Mikroanalytisches Labor Beller (Göttingen, Germany). Other elemental analyses were done on Elementar vario EL (Elementar, Germany).

The molecular modeling calculations were carried out by means of an Pentium II PC, 300 MHz, with the operating system LINUX, SuSE distribution 7.3,[19] Kernel vers. 2.4. The geometry and the conformation of the monomer units were optimized by means of quantum mechanical ab initio calculations using the software package GAMESS[20] with the optional parameters of the restricted Hartree−Fock self-consistent-field method and the basis set 6-31G** (with diffuse orbitals: for H as +2p and for C, N, O, and F as +3s and +3p). Single polymer chain models were generated by own written software which is able to chain up different kinds of monomer units. Thus, it is possible to realize linear, hyperbranched, and perfectly branched polymers. The formation of connecting monomer units of 100 substituted ethylenes and maleimides was carried by an alternating polymerization based on a randomly chosen rotation angle of ±20°. Therefore, polymer chain models with random conformations could be obtained.[21]

Glass transition temperatures (T_g) and melting points (T_m) were determined on a DSC Q1000 (TA Instrument) over a temperature interval of −80 to 200 °C at a scan rate of ±20 K/min. The T_g's were determined using the half-step method from the second heating runs.

Wide-angle measurements were done by the X-ray diffractometer P4 (Bruker *axs* Karlsruhe) with Cu Kα radiation (monochromatization by primary graphite crystal) in transmission. The radial scattering field ($2\Theta \approx 1.8-40.5°$) was acquired by integration of the 2-dimensional scattering pattern received with a HiStar area detector (GADDS). Small-angle data were recorded by means of a 3-fold pinhole system (self-construction) equipped by a Rigaku rotating anode and applying Cu Kα radiation (monochromatization by primary OSMIC confocal optic) in transmission. The scattering range (radial: $2\Theta = 0.09 \ldots 3.7°$, corresponding to $d \approx 99 \ldots 2.4$ nm) has been produced in manner similar to WAXS by an area detection system HiStar/GADDS. On-line SAXS experiments with heating and cooling furnace procedures were carried out on the Polymer Beamline A2 at HASYLAB (DESY Hamburg) for a d value range of 1.8−33 nm.

The IR investigations were carried out with a Bruker IFS66 spectrometer equipped with a heatable Golden Gate Diamante ATR Unit (SPECAC). 100 scans for one spectrum were co-added at a spectral resolution of 4 cm^{-1}. The corresponding temperature for the desired measurement was controlled manually and set by 5 °C intervals for the annealing and cooling process. All spectra were baseline corrected. As expected, all bands showed lowered intensities after the annealing and cooling process.

Silicon wafers (2×2 cm^2) with a round hole of 1 mm in diameter (Sico Wafer GmbH, Jena, Germany) were used as substrates for the formation of the MI copolymer films. Before using, the silicon wafers were cleaned with a piranha solution (4:1 mixture of H_2SO_4 and H_2O_2) at 80 °C for 1 h, then the wafers were rinsed with deionized water for 30 min, blown dry with a nitrogen stream, and treated with hexamethyldisilazane vapor for 2 h.

Film Preparations. The silicon wafers had a native SiO_2 layer of approximately 2 nm. The polymer solutions of 2 wt % concentration in tetrahydrofuran for STMF, STMH, ODMF, ODMH, and ETMH and in hexafluoro-2-propanol for ETMF were filtrated through a 0.25 μm poly(tetrafluoroethylene) filter to remove particles just prior to its spin-coating. The spin time was 30 s at a spin speed of 2000 rpm. Then the films were transferred into a vacuum oven and dried at 40 °C and 9.3 mbar for additional 24 h. Annealing experiments for the films were performed at 9.3 mbar and 20 °C above T_g for 24 h.

To determine the polymer film thickness, ellipsometric measurements were performed at room temperature using a computer-controlled single-wavelength ellipsometer (SE 402, Sentech GmbH, Germany). A He−Ne laser ($\lambda = 632.8$ nm) was used as a light source. The angle of incidence (ϕ) was fixed at 70.0°. For each sample, the measurements was performed on four different places, and the results were averaged. The thickness (d) and refractive index (n) of a nonabsorbing single polymer film ($k = 0$) in air ($n_0 = 1$) were calculated from the ellipsometric angles Δ and Ψ according to the basic equation (1) of ellipsometry:[22]

$$\tan \Psi e^{i\Delta} = f(N_s, N_j, d_j, n_0, \lambda, \phi) \quad (1)$$

with $N = n - ik$ as complex refractive index of substrate (s) or layers (j), n the refractive index, k the extinction coefficient, j the number of layers, and n_0 the refractive index of the ambient medium.

SFM tapping mode measurements were carried out using atomic force microscopy of Nanoscope III (Digital Instruments, Santa Barbara, CA) at room temperature. A commercial silicon cantilever with a spring constant of 35 N/m and resonance frequency around 285 kHz were used. Unless stated otherwise, moderate force tapping mode with set point ratio γ_{sp} at 0.5−0.8 was employed to achieve good contrast in both height and phase images. Data analyses were carried out using specifically designed Digital Instruments software (version 5.12 Nanoscope software). The values of root-mean-square roughness (R_{ms}) were calculated over the whole captured film area (5×5 μm^2).

The advancing contact angles of water were measured by a sessile drop technique using axisymmetric drop shape analysis profile (ADSA-P) at 24.5 ± 0.5 °C. The water was supplied to the sessile drop from below the wafer surface through a hole in the middle by a motorized syringe device. By pumping the water slowly into the water drop (0.1−0.2 mm/min), a sequence of images are recorded. A least-squares algorithm with surface tension as one of the adjustable parameters is applied to fit the experimental drop profile to the theoretical drop profile according to the Laplace equation. The accuracy of advancing and receding contact angles obtained in this method is within ±0.3°. Details of this technique can be referred in the literature.[23] The contact angle measurements were carried out on three different samples, and the results were averaged.

AR-XPS measurements were performed employing an Axis Ultra (Kratos Analytical, Manchester, England), equipped with a monochromated Al Kα ($h\nu = 1486.6$ eV) X-ray light source of 300 W at 15 kV. The kinetic energy of the photoelectrons was determined with an hemispheric analyzer with a pass energy of 160 eV for wide scan spectra and 20 eV for high-resolution spectra. The polymer films were mounted on a sample holder and introduced in a separate preparation chamber which was directly connected with the spectrometer. The chamber was quickly evacuated to a base pressure no higher than 2.7×10^{-8} mbar. Then the samples were transferred to the analysis chamber of the spectrometer where the spectra were recorded. During all measurements, electrostatic charging of the sample was avoided by means of a low-energy electron source working in combination with a magnetic immersion lens. All the recorded peaks were shifted by the same value which was necessary to set the C 1s peak to 285.0 eV.[24] The polymer surface was investigated by three different takeoff angles Θ (0°, 60°, and 75°, corresponding to the information depths of 8, 6, and 2 nm). Θ is defined as the angle between the sample surface normal and the optical axis of the photoelectron spectrometer. The sample information depth (d) can be approximated according to the equation $d = 5\lambda \cos \theta$, where λ is the mean free path of photoelectron. The resulting quantitative elemental compositions were determined from peak areas using experimentally determined sensitivity factors and the spectrometer transmission function. Spectrum background was subtracted according to the Shirley method.[25] The high-resolution spectra were dissected by means of the spectra deconvulsion software. The parameters of the component peaks were their binding energy, height, full width at half-maximum, and the Gaussian−Lorentzian ratio.

Results and Discussion

Molecular modeling calculations for the alternating MI copolymers with a polymerization degree of 100,

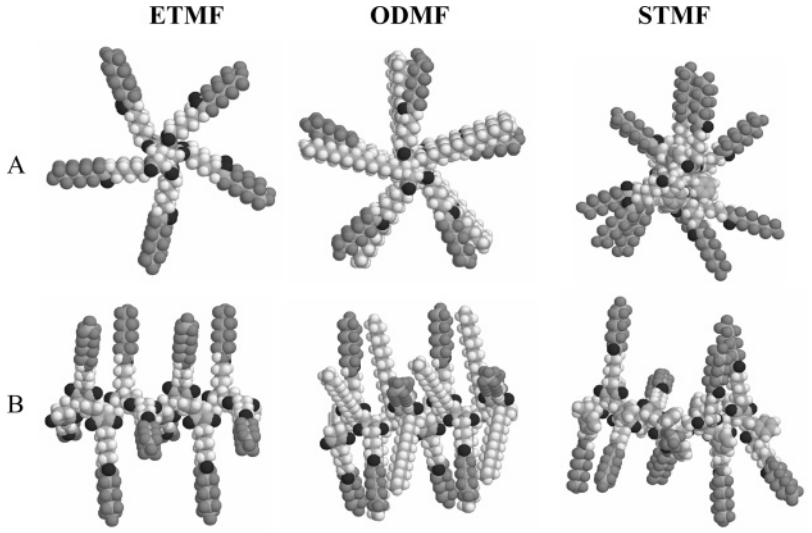

Figure 1. View (A = view in the direction of the main chain and B = side view) onto 10 maleimide/alkene repeating units for ETMF, ODMF, and STMF by molecular modeling calculation based on a helical chain conformation caused by *all-trans* configuration of the repeating units.

using the repeating units ethene-*N*-(R_f)alkylmaleimide, styrene-*N*-(R_f)alkylmaleimide, and octadecene-*N*-(R_f)-alkylmaleimide, were done to obtain fundamental aspects for the explanation of the experimental results. Thus, wormlike shapes with extended (R_f) side chains, presented for all MI copolymers (Supporting Information), are recognizable possessing helical chain conformation based on alternating polymerization walk with predefined *trans*-configuration of the maleimide ring for the repeating units. Ten calculated maleimide/alkene repeating units for ETMF, STMF, and ODMF are also depicted in Figure 1 (A = view in the direction of the main chain and B = side view).

For ETMF an interchain space can give the possibility of side chain interdigitation resulting in highly ordered structures. In the case of ODMF two different side chains with similar length scale are attached on the backbone. Therefore, it is assumed that the interchain space is not enough to initiate side chain interdigitation for the realization of layered main chains. The interchain space for STMF lies between ETMF and ODMF caused by the shorter, but voluminous, phenyl ring. The aliphatic counterparts ETMH, STMH, and ODMH may behave similar to the fluorinated copolymer ETMF, STMF, and ODMF.

The chain conformation for the MI copolymers in this paper is considered as helical-like state. This means that the chain conformation in the solid will not be a perfect one, but preferably with the main chain surrounded by completely/partly extended (R_f) side chains with the possibility of interchain packing.[26,27]

Bulk Properties. The transition temperatures and enthalpies of the MI copolymers are summarized in Table 2 determined by DSC. As expected, the T_g value for the styrene copolymers STMF and STMH are higher than those of the corresponding ethene and octadecene copolymers ETMF, ETMH, ODMF, and ODMH. The T_g values of ETMF, STMF, and ODMF are higher compared with the corresponding aliphatic counterparts ETMH, STMH, and ODMH which may be caused by the stronger interaction of the R_f side chains themselves suppressing a faster molecular motion of the MI main chains. Also, the R_f-NH-amide group of ETMF, STMF, and ODMF will make a contribution to increase the glass transition temperatures due to H-bonding interactions.

Table 2. Transition Temperatures and Enthalpies of Poly(alkene-*alt*-*N*-(*n*-(R_f)alkyl)maleimide) Copolymers Determined by DSC

	second heating			cooling after first heating	
polymer	T_g (°C)	T_m (°C)	ΔH_m (J/g)	$T_{c,m}$ (°C)	ΔH_c (J/g)
ETMF	100	163	3.3	152/157	−3.2
ETMH	57	−38	11.8	*a*	*a*
		85	3.7	74	−3.7
STMF	113				
STMH	70				
ODMF	63	−22	1.9	*a*	*a*
ODMH	∼30	−22	20.9	*a*	*a*

[a] Not calculated because of program temperature deviates from sample temperature below −20 °C at a cooling scan of 20 K/min.

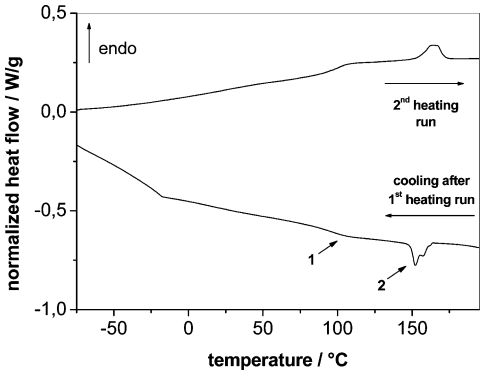

Figure 2. DSC thermogram of ETMF at the cooling run and the second heating run.

For ETMF an exothermic peak at 152/157 °C could be observed from cooling run after first heating run and a melting peak on the second heating run at 163 °C (Figure 2). This means that a transition from ordered to disordered state in the bulk at 163 °C may exist. Different fluorinated side chains with the shortest length scale of perfluoroalkyl segments in polymers behave similar to ETMF.[28,29] The aliphatic counterpart of ETMF, ETMH, shows two endothermic transitions at −38 °C, belonging to the melting of the aliphatic side

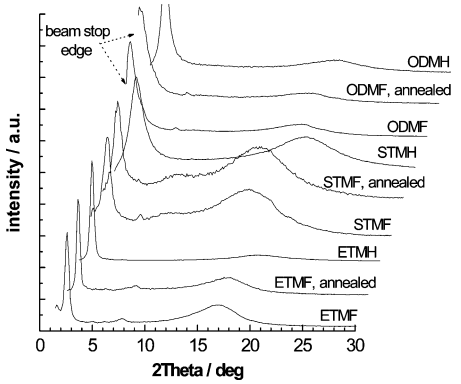

Figure 3. WAXS pattern of ETMF, STMF, ODMF, ETMH, STMH, and ODMH with different (R_f—) side chains.

Table 3. *d* Value Obtained by WAXS Experiments for MI Copolymers

polymer	*d* value[a] (nm)	*d* value[b] (nm)
ETMF	3.42	3.50
ETMH	3.21	*c*
STMF	2.90	3.02
STMH	2.48	*c*
ODMF		
ODMH	2.98	*c*

[a] Measured at room temperature. [b] Measured at room temperature after annealing at 20 °C above T_g for 24 h. [c] Not determined.

chains, and at 85 °C, attributing to the ordered/disordered transition of the material in the bulk.

ODMF shows an extremely reduced melting behavior of the aliphatic side chains at −22 °C in opposite to ODMH. It can be concluded that a preferentially weak phase separation between the R_f side chains and the hexadecyl side chains in ODMF occurs caused by the alternating substitution pattern of the side chains and the helical-like state of the main chain in ODMF. In other words, the similar chain lengths of the alternating side chains suppress preferred side chain crystallization and melting. In contrast to ODMF, acrylate copolymers based on stearyl methacrylate and 1*H*,1*H*,2*H*,2*H*-perfluorodecyl acrylate possess two melting peaks coming from different ratio of the used (meth)acrylate in polymerization.[29] For this observation, the existence of microphase separation between the side chains in the bulk was responsible due to the realization of block sequences of each acrylate monomer during copolymerization.[29]

The results of wide-angle X-ray diffraction experiments (WAXS) of the MI copolymers are shown in Figure 3. As one important aspect can be extracted that all MI copolymers, except ODMF, are materials with layer structures. The measured layer distances, corresponding to backbone−backbone distance, are given in Table 3. It is recognizable that ETMF and STMF with the same fluorinated side chain result in different *d* values (3.42 vs 2.9 nm) and their aliphatic counterparts ETMH and STMH (3.21 vs 2.48), too. The different length scales of extended R_f side chains and the second side chains in STMF, STMH, ODMF, and ODMH are shown in Figure 4 to support the following discussion about the WAXS results.

Under the assumption of helical-like chain conformation attached with extended (R_f) side chains for the investigated MI copolymers, a detectable *d* value for ODMF by WAXS is not possible due to the beam stop

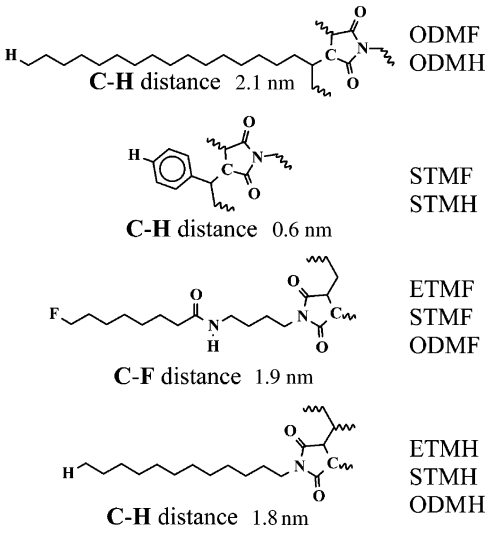

Figure 4. Length scale with extended R_f side chains and aliphatic/aromatic side chains in ETMF, STMF, ODMF, ETMH, STMH, and ODMH.

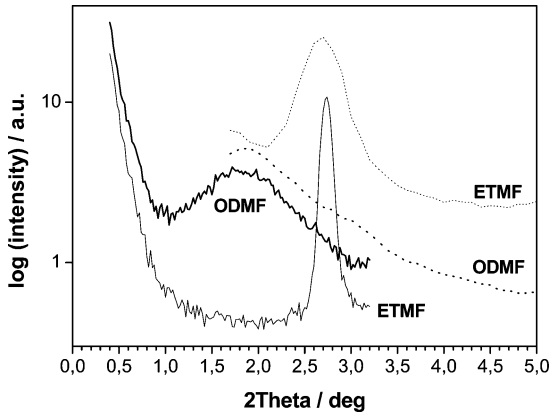

Figure 5. Scattering behavior of ODMF and ETMF at small angles measured by SAXS (solid lines) and WAXS (dotted lines) devices with different angular resolution.

edge. Additional SAXS investigations of ODMF revealed that only a very broad signal from 3.5 to 7.5 nm (Figure 5) could be observed. The broad signal indicates that ODMF has a variable layer distance caused by no real interchain space for side chain interdigitation and no real phase separation of the two different side chains, but with similarly extended side chain length. In other words, only if, e.g., the ODM backbone possesses longer fluorinated side chain, then it will be possible to receive a better phase separation with possible side chain interdigitation.

The wormlike shape of ETMF obtained from the molecular modeling calculation indicated that enough space between the R_f side chains of ETMF is given to initiate an interdigitation of the R_f side chains of another main chain. Therefore, a layer distance *d* of 3.4 nm between two main chains can be explained, but with a low degree of side chain interdigitation. Additional temperature-dependent SAXS investigation for ETMF was carried out to prove defined layer distance *d* at higher temperature, too. The annealing process from room temperature up to 200 °C and the reverse process are depicted in Figure 6.

Two transition states can be observed for the annealing process: (1) Up to the T_g value (∼100 °C) the layer distance has a weakly increasing behavior, and then a

Table 4. Assigned Wavenumbers of NH Stretching and Amide II Bands after Heating and Cooling Run for the Determination of H-Bonding Interaction of ETMF, STMF, and ODMF Obtained from Temperature-Dependent ATR-IR Spectroscopy

		position of band maximum (cm^{-1})		
sample	IR band	at 35 °C before heating	at elevated temperature	at 35 °C after cooling
ETMF	ν_{NH}	3320.4	3349.0 (180 °C)	3323.7
	amide II	1540.3	1532.4 (180 °C)	1540.8
STMF	ν_{NH}	3323.6	3340.6 (170 °C)	3330.4
	amide II	1541.2	1534.0 (170 °C)	1541.2
ODMF	ν_{NH}	3326.3	3334.5 (120 °C)	*a*
	amide II	1544.1	1540.0 (120 °C)	*a*

[a] Not determined.

stronger decreasing of the layer distance starts. (2) At ~150 °C the layer reflection disappears, and only a disordered state at higher temperatures exists. Both transitions are also observed during the cooling process, but in an opposite appearance. The high melting peak for a ordered/disordered transition at 163 °C, obtained from DSC (Figure 2), correlates well with the observation by temperature-dependent SAXS. In general, ETMF possesses a defined layered structure over a broad temperature range. This behavior of ETMF in solid/molten state resembles previously described fluorinated side chain polymer.[30]

STMF possesses a layer distance d of 2.9 nm. This value is lower than that of ETMF. A possible reason for the lowest layer distance d within the series of MI copolymers with R_f side chains can be that the required space for the phenyl substituent induces a closer arrangement of the main chains. This reveals also another organization of the fluorinated side chains in the bulk of STMF. Therefore, the assembled molecules of STMF do not show an additional melting peak at higher temperatures like ETMF by DSC. For the aliphatic counterparts ETMH and STMH the same side chain alignments in the bulk phase exist compared to ETMF and STMF. In the case of ODMH the calculated d value of 3 nm indicates that a defined layer distance will be supported by the presence of only one kind of side chain in opposite to ODMF.

H-bonding interactions of the amide group in the side chain for the MI copolymers ETMF, STMF, and ODMF were observed by temperature-dependent ATR-IR spectroscopy. The assigned wavenumbers at room temperature and different annealing temperatures for the NH-stretching band and the amide II band are outlined in Table 4.

In all cases the NH-stretching band shifted to higher wavenumbers and the amide II band shifted to lower wavenumbers during the annealing process. These are typical band shifts which indicate the weakening of the average strength of hydrogen bonds between the amide groups with increasing temperature.[31] Upon cooling to 35 °C, the nearly same starting wavenumber for both bands could be achieved for ETMF and STMF. Figure 7 shows the band shifts of the NH groups in dependence on the temperature in ETMF as an example for the breaking of H-bonding in the bulk of alternating maleimides. Interestingly, the annealing process reveals that the graph of the ν_{NH} band behaves similar to the second heating run of the DSC measurement. This means that a stepwise increase of the wavenumbers for the ν_{NH} band is recognizable, including nearly plateau formation after achieving the glass transition temperature and a great jump of the wavenumber at approximately 160 °C during the melting process of ETMF. For ETMF it can be concluded that the change of the H-bonding interaction of the perfluorinated amide group in the fluorinated side chain is conform to the thermal properties obtained from DSC and the formation of stable layer structures up to 150 °C observable by temperature-dependent SAXS. In general, the ATR-IR results reveal that the H-bonding interactions in ETMF, STMF, and ODMF have also an influence on their bulk properties, resulting in higher glass transition temperatures compared to the aliphatic counterparts ETMH, STMH, and ODMH.

Film and Surface Properties. The thickness of spin-coated films of the MI copolymers before and after annealing was determined in the range of 55−100 nm by ellipsometry. Highly stable films for the MI copolymers were received for both cases, the virgin and annealed (20 °C above T_g for 24 h) process.

To receive additional information about the surface topography of virgin and annealed copolymer films, the surfaces of the spin-coated films for ETMF, STMF, ODMF, ETMH, STMH, and ODMH were investigated by AFM tapping mode. The corresponding surface roughness parameters R_{ms} of each film are presented in Table 5. In all cases homogeneous films and smooth surfaces were prepared. The surface of ETMF is shown in Figure 8a,b as an example for the MI films. Small holes are recognizable at the virgin ETMF films (Figure 8a). After the annealing process the surface of the ETMF film resulted in terrace-like plateaus. The cross-section analysis of the ETMF surface shown in Figure 8b reveals an edge height of about 4 nm. All other edge heights are in the range of 3.5−4.0 nm, too. The determined edge height seems to be conform with the layer distance d of 3.15−3.50 nm obtained by WAXS and (temperature-dependent) SAXS. This means that a well-ordered stacking of ETMF molecules is also given in thin spin-coating films and on the film surfaces due to well-established side chain organization. In other words, ETMF possess self-enhanced formation of layered structures in the bulk and on the surfaces. Furthermore, only for ETMF holes could be observed in their films.

The characterization of the surface-energetic properties of the MI copolymer surfaces was done by ADSA-P to receive a better insight into the constancy of the advancing contact angles indicating the compatibility with Young's equation. The results of the advancing contact angles for all MI copolymers are summarized in Table 6. The surfaces of MI copolymers with *n*-dodecyl side chain possess θ_A values from 100° to 105.5°. Here, STMH with the main chain poly(styrene-*alt*-maleimide) shows the lowest θ_A value and ETMH and ODMH show explicit higher θ_A values. Within the aliphatic series the increasing hydrophobicity of the MI copolymer surfaces is governed by the main chain in the following order: poly(styrene-*alt*-maleimide) < poly(ethene-*alt*-maleimide) ≈ poly(octadecene-*alt*-maleimide). In both cases, virgin and annealed films, ODMH and ETMH possess a more preferred organization of the CH_3 groups on the upper layer of the surface due to a dense packing of the aliphatic side chains.

In ref 5b surface properties of densely packed *n*-dodecyl side chain on MI copolymers based on main chain poly(styrene-*alt*-maleimide) and poly(propene-*alt*-

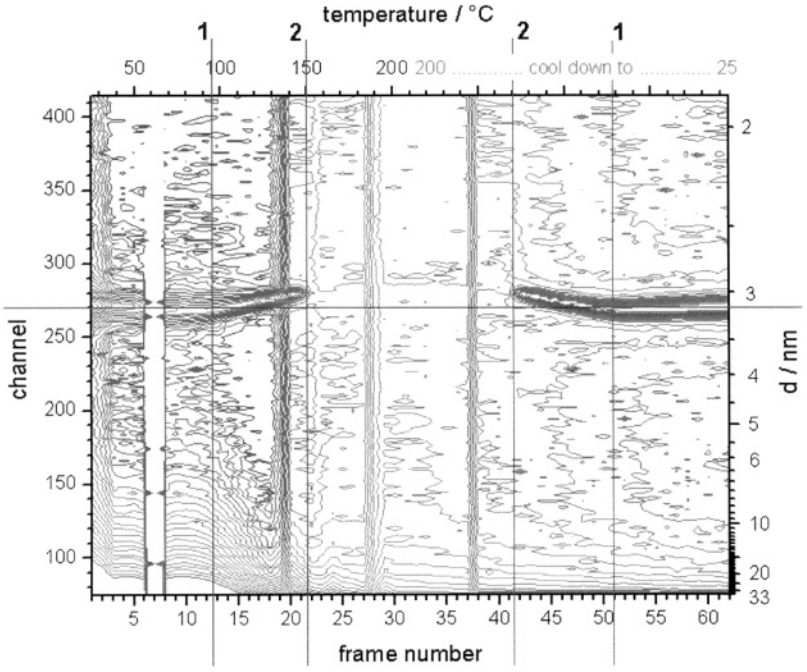

Figure 6. Temperature-dependent SAXS pattern (intensity contour plot) of ETMF sample obtained during heating from 20 to 200 °C and subsequent cooling with rate of 3 K/min. The transitions at 95 and 150 °C correspond to observed ones in DSC (1 and 2 in Figure 4).

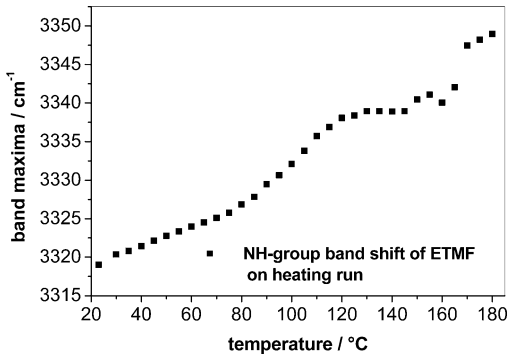

Figure 7. Maximum shifts of the NH-stretching band of ETMF in dependence on the temperature by ATR-IR.

Table 5. Surface Roughness R_{ms} of ETMF, STMF, ODMF, ETMH, STMH, and ODMH Films by AFM Using Tapping Mode

layer	$R_{ms}{}^a$ (nm)	$R_{ms}{}^b$ (nm)	layer	$R_{ms}{}^a$ (nm)	$R_{ms}{}^b$ (nm)
ETMF	2.14	3.76	STMH	0.17	0.29
ETMH	0.26	4.36	ODMF	3.04	1.03
STMF	3.15	4.55	ODMH	0.34	0.26

[a] Virgin film. [b] Annealed film.[a,b] Lateral dimension 5 × 5 μm^2 for R_{ms}.

maleimide) are assumed compared to literature examples. The resulting hydrophobicity of these MI surfaces are similar to STMH in this study. Therefore, a revised view of densely packed *n*-dodecyl side chains with more perfectly organized CH_3 groups on the top of the surface can be established within the series of alternating MI copolymers based on main chains with slightly increasing θ_A values for water: poly(styrene-*alt*-maleimide) ≅ poly(propene-*alt*-maleimide) < poly(ethene-*alt*-maleimide) ≈ poly(octadecene-*alt*-maleimide).

For the virgin and annealed ETMF and ODMF films very hydrophobic surfaces could be obtained resulting

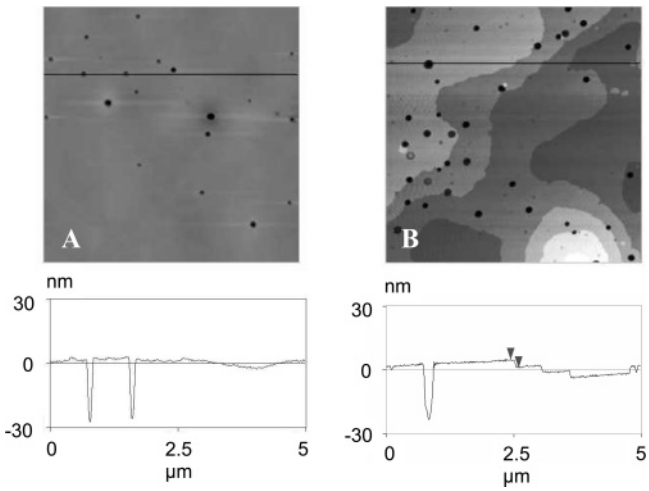

Figure 8. AFM images of ETMF film before annealing (A) and after annealing (B) for 24 h at 115 °C. Increased hollow formations after annealing is observed. Cross-sectional analyses are shown for the image (A) and (B). Terrace-like formation of the surface in (B) was determined with average edge heights of 3.5−4.0 nm presented by the two arrows.

Table 6. Summary of Low Rate Dynamic Advancing Contact Angles of Water on ETMF, ETMH, STMF, STMH, ODMF, and ODMH Surfaces

surface	θ_A/deg[a]	θ_A/deg[b]
ETMF	118.2 ± 0.5	120.4 ± 0.9
ETMH	104.7 ± 0.6	105.2 ± 0.8
STMF	106.8 ± 1.7	114.4 ± 1.7
STMH	99.8 ± 0.7	102.1 ± 0.3
ODMF	120.0 ± 0.2	118.0 ± 0.7
ODMH	105.5 ± 0.8	106.9 ± 0.6

[a] Virgin film. [b] Annealed film.

in θ_A values in the range of 120°. It can be assumed that ETMF and ODMF possess preferentially organized CF_3 groups on the top of the surfaces. For ETMF a slightly increasing θ_A is detectable after annealing.

Table 7. Summary of Solid Surface Tension of ETMF, ETMH, STMF, STMH, ODMF, and ODMH Calculated from Mean Advancing Contact Angles of Water (γ_{lv} = 71.9 mJ/m^2) for Virgin (A) and Annealed (B) Films

surface	γ_{sv} (A), mJ/m^2	γ_{sv} (B), mJ/m^2
ETMF	12.22	11.08
ETMH	19.78	19.49
STMF	18.56	14.25
STMH	23.18	21.75
ODMF	11.29	12.32
ODMH	19.31	18.46

Contrary to this case, the annealed ODMF surface showed a slight decrease of θ_A. The received θ_A results for ETMF and ODMF are similar/equal to described literature results of fluorinated side chain containing polymers.[28−30,32] Semifluorinated side chains in block copolymers showed high θ_A values for water between 120° and 123°, resulting in critical surface tension of 8.0 mN/m, obtained from the Zisman plot.[32]

For STMF the styrene-*alt*-maleimide main chain does not allow preferentially organized CF_3 groups on the surface as found for ETMF and ODMF. Here, non-densely packed R_f side chains are present. The different alignment of the R_f side chain in STMF compared to ETMF and ODMF is reflected again by the lower layer distance d in WAXS experiments, meaning a different organization of the R_f side chains in the bulk phase of STMF.

The STMF surface shows an increase in θ_A values from approximately 107° to 114.4° after the annealing process at 20 °C above T_g for 24 h. This is an indication for a denser alignment of the R_f side chain, meaning a higher content of CF_3 groups at the surface.

The advancing contact angles of the MI copolymer surfaces were used to calculate the solid surface tensions γ_{sv} using the equation of state for interfacial tensions.[17] The results are given in Table 7 for different MI copolymer surfaces. In this connection, there was the assumption to realize more densely packaged R_f side chains with closer arrangement of CF_3 groups on the top of the surface after annealing process. The resulting average values of solid surface tensions for annealed R_f-MI copolymer surfaces gave following series starting from the highest value: 14.25 mJ/m^2 for STMF, 12.32 mJ/m^2 for ODMF, and 11.08 mJ/m^2 for ETMF. Here, the surface of MI copolymers ETMF, STMF, and ODMF with the same R_f side chain is dominated by the different state of enriched and exposed CF_3 groups. Especially, for STM surface the highest decrease of surface tension could be realized compared to ETMF surface after annealing process. Only the annealed ODMF surface shows a slightly increase of the surface tension. In other words, the wettability of the alternating MI copolymer films is influenced by the main chain substitution pattern of the copolymers. The feature of the main chain in STMF results in higher solid surface tension values compared to ETMF and ODMF. In general, the wettability of the MI copolymer surfaces is tuned by the main chain and the attached side chain.

AR-XPS was used to investigate the surface composition due to its good surface sensitivity and capability of providing chemical bonding information. Figure 9 presents the high-resolution XPS spectrum of the ODMF surface. Here, a complete peak assignment could be realized for the chemical substructure of the fluorinated side chain, including the maleimide ring. The analysis of the fluorine content at 8 nm information depth,

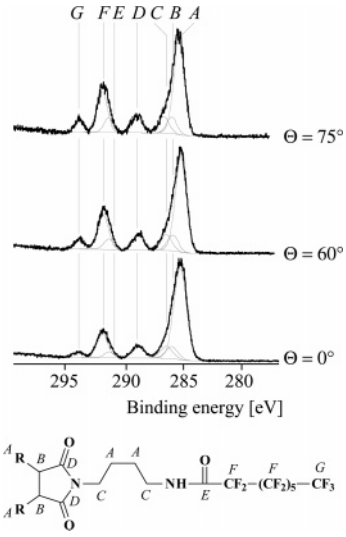

Figure 9. High-resolution C 1s photoelectron spectra of sample annealed ODMF film recorded in dependence on the tilt angle Θ. Different carbon species in the polymer chain cause the component peaks A, B, C, D, E, and F.

Table 8. F/C Ratio at Different Information Depth Determined by Angle-Resolved XPS and Theoretical/Found F/C for ETMF, STMF, and ODMF Compared with Their Solid Surface Tension γ_{sv}

	F/C ratio					
	information depth			bulk		
film	8 nm	4 nm	2 nm	theoretical	found[c]	γ_{sv} (mJ/m^2)
ETMF[a]	0.745	0.750	0.747	0.833	0.737	12.22
STMF[a]	0.510	0.497	0.516	0.625	0.610	18.56
ODMF[a]	0.440	0.618	0.715	0.441	0.421	11.29
ODMF[b]	0.391	0.508	0.537	0.441	0.421	12.32

[a] Virgin film. [b] Annealed film. [c] Used elemental and fluorine analysis.

presenting more than a monolayer of the investigated MI copolymer, outlines a confirmation of the shown F analysis of ETMF, STMF, and ODMF in Table 1. Also, the F/C ratio at 8 nm information depth is similar to the found F/C ratio for the bulk shown in Table 8.

The AR-XPS investigations allow to observe a difference composition of atomic compounds on the outermost surface of spin-coated films in dependence on used information depth from 8 to 2 nm. The F/C ratio of the polymer surface for films and theoretical/found bulk ratio of the F/C ratio for the MI copolymers compared with their solid surface tension are summarized in Table 8. Coming from 8 to 2 nm information depths on the virgin surface, only ODMF shows an increased F/C ratio at the outermost layer of the surface compared to uniform F/C ratio for the ETMF and STMF surface of polymer films. At 2 nm information depth the F/C ratio for ODMF is similar to that for ETMF. Therefore, it can be assumed that the R_f side chains of ODMF may be preferentially aligned in the outermost layer of the surface. For the annealed ODMF film from 8 to 2 nm information depth a lower increase of F/C ratio is determined.

The investigation of the surfaces by AR-XPS for ODMF surfaces confirms the received results obtained from contact angle measurements. Here, the surface arrangement of virgin ODMF surface shows a nearly perfect phase separation between the aliphatic and fluorinated side chains on the top of the surface. The virgin layer of ODMF may reflect the frozen state of the

Scheme 2

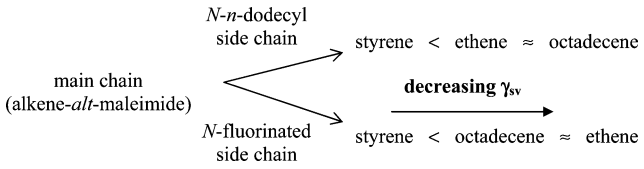

spin-coating process. This process allows the phase separation between aliphatic and fluorinated side chains in ODMF and the orientation of the R_f side chain to the upper surface. The thermal treatment of the spin-coated film of ODMF transfers the frozen state of phase-separated side chains into more alternating arrangement comparable with the bulk phase. By this, the low decrease of θ_A by ADSA-P in Table 6 can be explained.

For the films of ETMF, STMF, and ODMF, a direct correlation was found between the fluorine content in the outermost surface region and the solid surface tension calculated from the advancing water contact angle (Table 8).

Conclusions

It can be stated that the origin aim, enriched exposition of CH_3 and CF_3 group surfaces, was realized due to the influence of used main chain with attached aliphatic and fluorinated side chain. This point is based on preferentially densely packaged side chains on the outermost surface. The following structure−property relationships can be postulated: (1) The ETM main chain allows a relatively undisturbed side chain organization, resulting in highly enriched CH_3 and CF_3 group surfaces. (2) The STM main chain has also a phenyl substituent besides the attached side chains. Thus, lowest hydrophobicity and highest surface tension were determined due to no densely packaged side chains. This point is supported by the thermal properties possessing no side chain melting for STMH and no transition phase from ordered to disordered for STMF compared to ETMF. Also, the STM series has shorter layered structures, indicating another side chain organization than the ETM series. (3) The ODM main chain has two side chains (*n*-hexadecyl and *n*-dodecyl or fluorinated side chain). In the case of aliphatic ODM a higher density of aliphatic side chains results in highest hydrophobicity and lowest surface tension. For the fluorinated ODM main chain different surface properties are present. The virgin ODMF surface shows similar/slightly higher hydrophobicity like ETMF. The enrichment of CF_3 groups on the top of the surface was confirmed by XPS investigation. The annealed ODMF surface shows the reverse case compared to the virgin ODMF surface. On the basis of the same side chain length in ODMF, the bulk properties of ODMF give an indication that a reduced phase separation between the aliphatic and fluorinated side chain is assumed reflecting also a bulk-like ODMF surface after annealing process. The correlation between used main chain and attached side chain and their influence on deceasing solid surface tension values (γ_{sv}) on polymer surfaces is summarized in Scheme 2. Thus, a clear tendency is observable that the solid surface tension of MI copolymers are tightly correlated with the used main chains and side chain compositions.

Acknowledgment. We thank the Ministry for Education and Science of Germany (Grant 01RC0040) and the state saxonia for financial support. We thank Mrs. C. Lehmann for the synthesis of the MI copolymers and Mrs. Adam for carrying out the temperature-dependent ATR IR investigations.

Supporting Information Available: Presentation of molecular modeling calculation for ETMF, ETMH, STMF, STMH, ODMF, and ODMH. This material is available free of charge via the Internet at http://pubs.acs.org.

References and Notes

(1) Cubbon, R. C. P. *J. Polym. Sci., Part C* **1967**, *16*, 387.
(2) (a) Verbiest, T.; Samyn, C.; van Beylen, M.; Persoons, A. *Macromol. Rapid Commun.* **1998**, *19*, 349. (b) Gangadhara, S.; Ponrathnam, S.; Noel, C.; Reyx, D.; Kajzar, F. *J. Polym. Sci., Part A: Polym. Chem.* **1999**, *37*, 513.
(3) (a) Chiang, W.-Y.; Lu J.-Y. *Macromol. Chem. Phys.* **1994**, *195*, 591. (b) Chae, K. H.; Gwark, J. C.; Chang, T. *Macromol. Rapid Commun.* **1998**, *19*, 349.
(4) Kwok, D. Y.; Li, A.; Lam, C. N. C.; Wu, R.; Zschoche, S.; Pöschel, K.; Gietzelt, T.; Grundke, K.; Jacobsch, H.-J.; Neumann, A. W. *Macromol. Chem. Phys.* **1999**, *200*, 1121.
(5) (a) del Rio, O. I.; Kwok, D. Y.; Wu, R.; Alvarez, J. M.; Neumann, A. W. *Colloids Surf. A: Physiochem. Eng. Aspects* **1998**, *143*, 197. (b) Grundke, K.; Zschoche, S.; Pöschel, K.; Gietzelt, T.; Michel, S.; Friedel, P.; Jehnichen, D.; Neumann, A. W. *Macromolecules* **2001**, *34*, 6768.
(6) Lange, R. F. M.; Meijer, E. W. *Macromolecules* **1995**, *28*, 6768.
(7) (a) Gouzy, M. F.; Sperling, C.; Streller, U.; Salchert, K.; Böhme, F.; Voit, B.; Werner, C. *Polym. Prepr.* **2002**, *43*, 695. (b) Pompe, T.; Zschoche, S.; Salchert, K.; Herold, N.; Werner, C. *Biomacromolecules* **2003**, *4*, 1072.
(8) Yan, H.; Zhu, X. *J. Appl. Polym. Sci.* **1999**, *74*, 97.
(9) Fleš, D. D.; Golija, G.; Hace, D.; Vukovic, R.; Fleš, D. *Polym. Bull. (Berlin)* **1994**, *33*, 425.
(10) (a) Hendlinger, P.; Laschewsky, A.; Bertrand, P.; Delcorte, A.; Legras, R.; Nysten, B.; Möbius, D. *Langmuir* **1997**, *13*, 310. (b) Jeong, H.; Lee, B.-J.; Cho, W. J.; Ha, C.-S. *Polymer* **2000**, *41*, 5525.
(11) Kwok, D. Y.; Gietzelt, T.; Grundke, K.; Jacobasch, J.-H.; Neumann, A. W. *Langmuir* **1997**, *13*, 2880.
(12) Baltá-Calleja, F. J.; Ramos, J. G.; Barrales-Rienda, J. M. *Kolloid Z. Z. Polym.* **1972**, *250*, 474.
(13) Percec, V.; Schlüter, D.; Ronda, J. C.; Johansson, G.; Ungar, G.; Zhou, J. P. *Macromolecules* **1996**, *29*, 1464.
(14) (a) Roth, H.; Arnhold, M.; Rätzsch, M. *Acta Polym.* **1981**, *32*, 277. (b) Review for the general structure analysis of *alt*-maleic anhydride copolymers: Chitanu, G.-C.; Zaharia, L.-I.; Caprov, A. *Int. J. Polym. Anal. Charact.* **1997**, *4*, 1.
(15) (a) Komber, H. *Macromol. Chem. Phys.* **1995**, *196*, 669. (b) Komber, H. *Macromol. Chem. Phys.* **1996**, *197*, 343.
(16) Ha, N. T. H.; Fujimori, K.; Tucker, D. J. *J. Macromol. Sci., Pure Appl. Chem.* **1996**, *A33*, 1209.
(17) Kwok, D. Y.; Neumann, A. W. *Adv. Colloid Interface Sci.* **1999**, *81*, 167.
(18) Spelt, J. K.; Li, D. In *Applied Surface Thermodynamics*; Neumann, A. W., Spelt, J. K., Eds.; Marcel Dekker: New York, 1996; p 239.
(19) Bauer, B.; et al. *SuSE Linux 7.3 Manual*, ISBN 3-930-419-67-X, 1998.
(20) Schmidt, M. W.; Baldridge, K. K.; Boatz, J. A.; Elbert, S. T.; Gordon, M. S.; Jensen, J. H.; Koseki, S.; Matsunaga, N.; Nguyen, K. A.; Su, S.; Windus, T. L.; Dupuis, M.; Montgomery, J. A. *J. Comput. Chem.* **1993**, *14*, 1347.
(21) Friedel, P. "RESMAIN, Program for building linear and hyperbranched polymers with optional parameters choosing constitutional and conformational statistics", unpublished software, Inst. of Polymer Research Dresden, 1998−2003.
(22) Azzam, R. M. A.; Bashara, N. M. In *Ellipsometry and Polarized Light*; North-Holland Publishing Co.: Amsterdam, 1977; p 529.
(23) Grundke, K.; Bogumil, T.; Gietzelt, T.; Jacobasch, H.-J.; Kwok, D. Y.; Neumann, A. W. *Prog. Colloid Polym. Sci.* **1996**, *101*, 58.
(24) Beamson, G.; Briggs, D. In *High Resolution of Organic Polymers*; The Scienta ESCA 300 Database; J. Wiley & Sons: Chichester, 1992; ISBN 0-471-93592-1.
(25) Shirley, D. A. *Phys. Rev. B5* **1972**, *101*, 58.

(26) Remark of the authors: molecular modeling calculations reveal that the presence of *cis*-configurated succinimide rings in maleimide copolymers will also result in helical main chain conformation surrounded by side chains; unpublished results.
(27) Tsuwi, J.; Appelhans, D.; Kremer, F.; Zschoche, S.; Friedel, P. *Macromolecules* **2004**, *37*, 6050.
(28) Corpart, J. M.; Girault, S.; Juhué, D. *Langmuir* **2001**, *17*, 7237.
(29) de Crevoisier, G.; Fabre, P.; Leibler, L.; Tencé-Girault, S.; Corpart, J. M. *Macromolecules* **2002**, *35*, 3880.
(30) Gottwald, A.; Pospiech, D.; Jehnichen, D.; Häussler, L.; Friedel, P.; Pionteck, J.; Stamm, M.; Floudas, G. *Macromol. Chem. Phys.* **2002**, *203*, 854.
(31) Coleman, M. M.; Skrovanek, D. J.; Painter, P. C. *Makromol. Chem., Macromol. Symp.* **1986**, *5*, 21.
(32) Wang, J.; Mao, G.; Ober, C. K.; Kramer, E. J. *Macromolecules* **1997**, *30*, 1906.

MA0486492